A MINIATURE PSEUDO-MULTI-HOLE PRESSURE PROBE CALIBRATION

F. Ceyhun Sahin/Laboratory for Applied Mechanical Design (LAMD), Ecole Polytechnique Fédérale de Lausanne (EPFL), Switzerland

Jürg Schiffmann/Laboratory for Applied Mechanical Design (LAMD), Ecole Polytechnique Fédérale de Lausanne (EPFL), Switzerland

ABSTRACT

Flow behavior at the exit section of a compressor impeller is quite complex before the mixing is complete in the diffuser. In order to determine the slip factor and so the correct compression performance of the impeller, velocity vector distribution in the jet-wake region should be investigated accurately. Multi-hole probes are widely used to measure the flow speed and direction. Close to the impeller exit, diameter of the probe should be smaller than the blade trailing edge thickness. For a fast response data acquisition, the sensor should be located in the measurement point vicinity.

Those constrains, combined with the fact that probe should comprise more than one measuring holes, suggest impossible compactness for multi-hole probe measurements in a micro-compressor stage. A pseudo-multi-hole probe is designed to measure velocity vector at the exit of a micro-compressor impeller. Only one hole, with a dimeter equal to the inner diameter of the tube, is drilled in radial direction on a medical needle. The directional information is to be acquired by turning the probe around its axis. The probe is first to be calibrated for its response to steady flow direction. Then a transfer function is to be defined to finalize dynamic calibration of the probe.

NOMENCLATURE

A	Area
c	Speed of sound [m/s]
D	Tube diameter [mm]
Ea	Isentropic bulk modulus [kg/m·s^2]
f_{Darcy}	Friction factor
f	Frequency [1/s]
j	Imaginary unit
κ	Heat capacity ratio
L	Tube length [mm]
m	Mass [kg]
P, p	Pressure [bars]
R	Specific gas constant [J/kg.K]
T	Temperature [K]
t	Time [s]
u	Speed [m/s]
V	Volume [mm^3]
x, y	Distance [mm]
μ	Viscosity [Pa·s]
ρ	Density [kg/m^3]
ω	Frequency [rad/s]

Abbreviations

Re	Real
TF	Transfer Function

Subscripts

I, i	Imposed
M, m	Measured
n	Natural

INTRODUCTION

Compressor performance maps are results of time averaged pressure and temperature measurements at the inlet and exit section for different flow rates at different rotational speeds. On the other hand, loss mechanism studies require more detailed measurements on different components of a compressor.

Although the literature is rich in terms of empirical relations to calculate different loss mechanisms in compressors, in small-scale turbomachines flow behavior will deviate from the given empirical relations because of higher relative clearances and blade thickness blockage. The motivation of this study is to determine the slip factor in a micro-compressor. That requires a time resolved measurement of flow speed and angle at the impeller exit before the mixing is complete in the diffuser.

For a stationary observer at the blade trailing edge, a rotary unsteady flow field occurs because of jet and wake regions. In order to determine the slip factor and then the correct performance of the impeller, velocity vector distribution in the jet-wake region

should be investigated accurately as close to the blade trailing edges as possible.

Multi-hole probes are widely used to measure flow speed and direction. Close to the impeller exit, diameter of the probe should be smaller than the blade trailing edge thickness. Impeller of a micro-compressor will have a diameter of 10-20 mm and blade height of 0.5-1 mm at the exit section [1], [2]. Conventional probes are usually large scale to be directly used in such narrow channels. For fast response data acquisition, the sensor should be located in the measurement point vicinity. Those constrains, combined with the fact that probe should comprise more than one measuring holes, suggest impossible compactness for multi-hole probe measurements in a micro-compressor stage.

A pseudo-multi-hole probe is designed to measure velocity vector at the exit of a micro-compressor impeller. This probe comprises only one hole to measure total pressure and the probe is turned around its axis to imitate directional holes of a multi-hole-probe. That kind of pressure measuring probes, sometimes combined with temperature measurement, are previously used [3] -[6]. The uniqueness of this probe is its small diameter. Smallest probe diameter presented in previous studies is 0.8 mm [3]. The new probe is supposed to measure behind impeller blades with a thickness of 0.6 mm. A medical syringe needle is used to manufacture a pitot-tube as thin as the blades. Only one hole in radial direction is drilled on the needle. The hole diameter is equal to the inner diameter of the needle. The needle converted to a probe is sketched in Figure 8. The first step in calibration will be determining the map of pressure coefficient for the probe at different incidences with respect to the flow. Although it is possible to manufacture a probe with outer diameter equal to 0.6 mm, a commercial pressure transducer in such compactness does not exist. That will be the main reason for a long needle standing between the measurement point and the transducer diaphragm. The amplitude and the frequency of the pressure wave will be damped and delayed along the channel. With increasing tube length and decreasing hole diameter, the channel will start acting as a low pass filter. Next step in calibration will be determining the transfer function between the imposed pressure value and the value measured by the sensor.

TRANSFER FUNCTION MODEL TO ESTIMATE PROBE NATURAL FREQUENCY

There are several models to define the natural frequency of connections for the transducers. Organ pipe approach can be adopted for long tubes but the cavity volume, where the sensor is placed, plays an important role in the deviation from organ pipe model as the tube gets shorter. A short tube connected to a cavity is similar to a Helmholtz resonator. However if the tube volume is significant compared to the cavity volume, Helmholtz equation overestimates the natural frequency systematically, when compared to experimental result [5]. A qualitative comparison of organ pipe or Helmholtz resonator models prove the advantage of small cavity and low aspect ratio (L/D) tube for a higher resonance frequency. The frequency response of the measurement chain will be limited to 2/3rd of the connecting tubes natural frequency [7].

Allegret-Bourdon [8] used tubes with an aspect ratio more than 500 to filters fluctuations higher than 200 Hz. Everitt [3] also studied with a fast response probe at the end of a long tube (L/D ≈ 20 according to the available data). The natural frequency of the probe is given as 2.6 kHz and it is used for measurements at the exit of an impeller rotating faster than three times the probe natural frequency. That probe was used to measure average values correctly. The compressibility effects or friction losses inside the tube are not considered in the natural frequency calculations. Resulting natural frequency is approximately the Helmholtz resonance frequency of the sensor volume at the end of the tube [3].

Aspect ratio for the tube designed for this study is 20 and the Helmholtz resonating frequency for total volume of tube and cavity is 4.3 kHz.

Bergh-Tijdeman (B-T) model [9] is an alternative for systems which can be modelled in a series of Helmholtz resonators. In B-T model, the flow in the tube is assumed viscous and laminar. There is no flow velocity in the volume but the air is compressed and membrane deflection is also taken into account. The robustness of this model for system natural frequency calculation is studied and validated

with experiments in comparison with Helmholtz resonant frequency [7] and it is referred by sensor manufacturers [7], [10]. Experimental investigations of Paniagua et al. [11] on the other hand, showed that Bergh-Tijdeman (B-T) model also overestimates the natural frequency. What is missing in the model is the head loss through the tube due to friction.

An alternative model is derived solving the dynamic system equation for the air mass filling the tube, compressed in the volume and damped because of the viscous friction on the tube walls (Figure 1). That approach suggests a resonance frequency more conservative than that from B-T model. Dynamic calibration of the probe will help whether or not to adopt this new model to estimate the system resonance frequency. Once the model is validated with experiments, it will be possible to extend dynamic calibration data to different tube lengths or diameters.

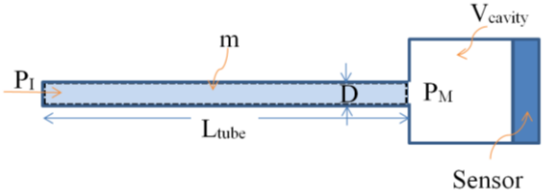

Figure 1 Probe interior geometry sketch

Total head loss across the tube will be

$$\Delta p = f_{Darcy} \frac{L_{tube}}{D} \rho \frac{c^2}{2} \qquad \text{Eq.1 a}$$

for compressible flow propagation. Force balance on the mass (m) is

$$P_I \cdot A_{tube} - \Delta p \cdot A_{tube} = m \frac{dc}{dt} + P_M \cdot A_{tube} \qquad \text{Eq.1 b}$$

Pressure in the cavity increases in time because of mass flow

$$P_M(t + \Delta t) = \frac{RT}{V}\left(m(t) + \frac{dm}{dt} \cdot \Delta t\right) \qquad \text{Eq.1 c}$$

Speed of compressible flow across the tube can be expressed in terms of pressure variation inside the cavity

$$c = \frac{dP_M}{dt} \cdot \frac{V}{A_{tube} \rho RT} \qquad \text{Eq.1 d}$$

Bulk modulus of the gas is $E_a = \rho c^2$. If a pressure pulse of $P_I = p_i \cdot e^{j\omega t}$ is imposed, pressure inside the cavity will fluctuate at the same frequency with a lag; $P_M = p_m \cdot e^{j(\omega t - kx)}$. Arranging Eq.1 b with geometrical parameters and gas properties results in

$$\frac{P_I}{P_M} = \frac{p_i}{p_m} \cdot e^{jkx}$$

$$TF = 1 + j \cdot \omega \cdot \frac{L_{tube} V \kappa}{E_a A_{tube}} \cdot \frac{8\mu\pi}{A_{tube}} - \rho \frac{L_{tube} V \kappa}{E_a A_{tube}} \omega^2$$

Eq. 1

The magnitude is the pressure damping and the angle is the phase lag. Imaginary component is a result of pressure loss through a pipe for laminar flow. Real component can be written in terms of resonating frequency in case system is not over-damped

$$\mathrm{Re(TF)} = 1 - \frac{\omega^2}{\omega_n^2} \qquad \text{Eq. 2}$$

Note that resonating frequency is very similar to Helmholtz resonance definition with tube volume added up to the cavity volume.

$$\omega_n = \sqrt{\frac{E_a / \kappa \, A_{tube}}{\rho L_{tube} V_{total}}} = c \sqrt{\frac{A_{tube}}{\kappa L_{tube} V_{total}}} \qquad \text{Eq. 3}$$

Comparison of this new model with previously mentioned models is in Figure 2. Models are compared for the probe geometry designed for this study. Resonating frequency estimations for the given tube length are close for three models: B-T, Helmholtz and the new model. New model is more sensitive to increasing tube length than the other models and resonating frequency estimation is more conservative for longer tubes.

A comparison of Eq. 1 for different D/L ratios in Figure 3 shows that for very thin tube (D = 0.15 mm) system is over-damped although this is not the case for a larger tube with the same D/L. Constant channel lengths are plotted with same dash. Longer the tube, lower the gain and resonating frequency, if the system is not over-damped. For excitations higher than 1 kHz, there is a risk for the system to resonate. For a tube of 7 mm length, among the cases plotted here, resonating frequency is

between 3 kHz and 10 kHz for tube diameters between 0.15 mm and 1 mm.

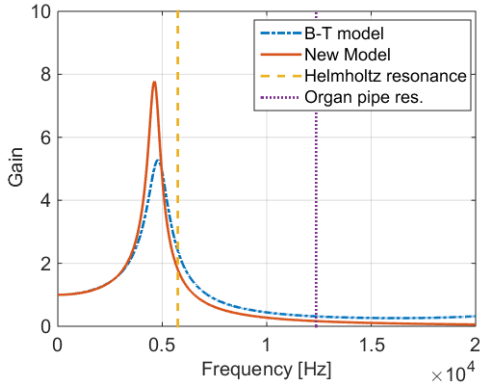

Figure 2 Transfer function models comparison for D = 0.35 mm, L = 7 mm and sensor cavity 1.27 mm^3

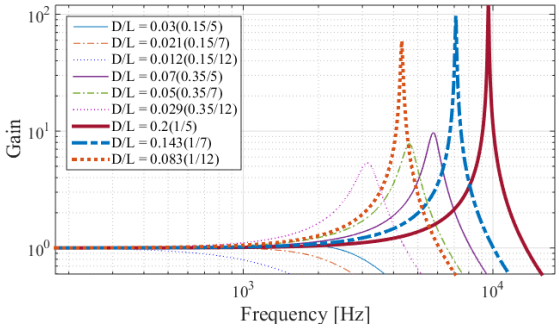

Figure 3 Transfer functions according to the new model for varying D/L, cavity volume of 1.27 mm^3

Cavity volume where the sensor is installed has also significant effect on the transfer function. System response to tube dimensions and cavity volume are investigated to determine the dominancy of parameters. In the plots of Figure 4 to Figure 6, a parametric study for the effects of tube geometries on the transfer function is summarized. Transfer functions are shown on the top plots. 2/3 of the resonating frequencies are marked on these plots. A probe will detect fluctuations up to half of the cut-off frequency accurately. Plots at the bottom show the frequency and corresponding gain for detectable values, which are also shown in dashed lines on the transfer function plots.

A brief look on these plots shows that the tube length and the cavity volume should be kept as small as possible where the tube diameter should be increased to assure higher cut-off frequencies. In the given range of probe dimensions, sensitivity to tube diameter and cavity volume varies more significantly than to tube length. One should note that increasing the tube diameter will require larger outer diameter of the tube and this will result in more blockage in the flow.

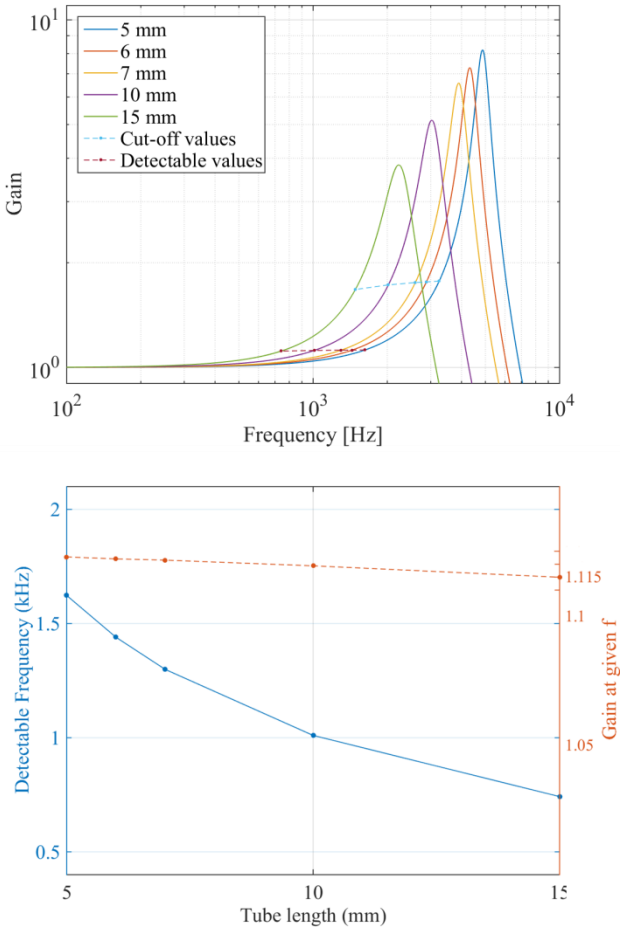

Figure 4 Truong model transfer functions for D = 0.35 mm and 1.27 mm^3 cavity, varying tube length (top); evolution of detectable frequency and the gain with tube length (bottom)

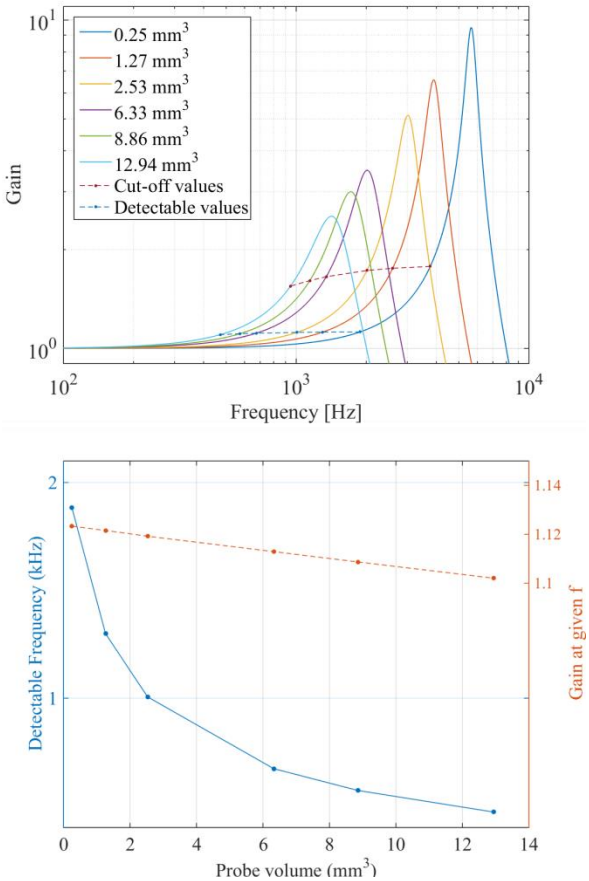

Figure 5 Truong model transfer functions for D = 0.35 mm and L = 7 mm, varying cavity volume (top); evolution of detectable frequency and the gain with probe volume (bottom)

Variation of cut-off frequency with respect to tube diameter versus length is summarized in Figure 7 for a fixed cavity volume. Lines of constant aspect ratio are added on the plot to emphasize the existence of an optimum in terms of absolute values for a given L/D. Keeping the aspect ratio fixed can sustain a high cut-off frequency up to a certain point. After that limit, increased tube length cannot be compensated with an increased tube diameter and cut-off frequency gets less sensitive to tube diameter. That means the volume of the cavity is not significant with respect to the total volume of the tube and the system behavior is more similar to an organ pipe.

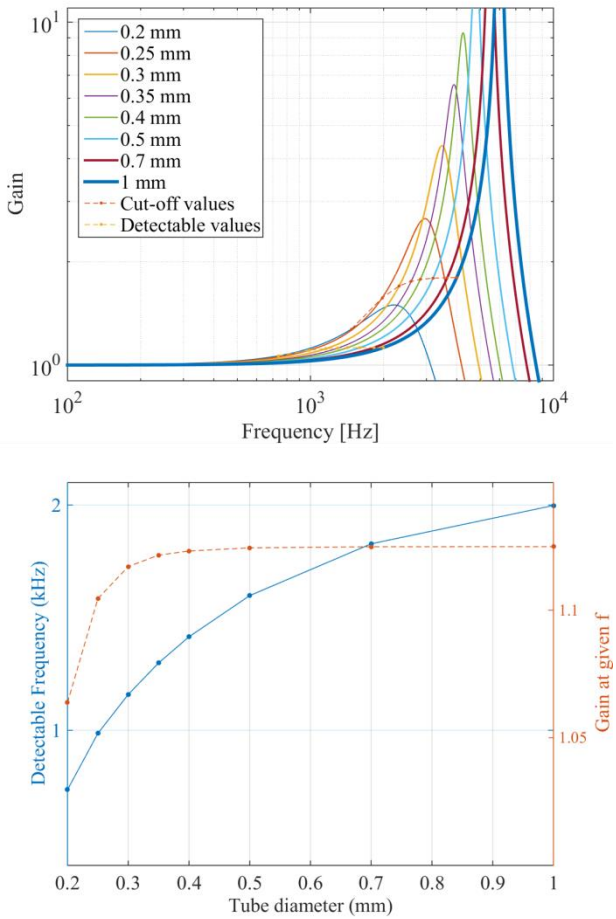

Figure 6 Truong model transfer functions for L = 7 mm and 1.27 mm³ cavity, varying tube diameter (top); evolution of detectable frequency and the gain with tube diameter (bottom)

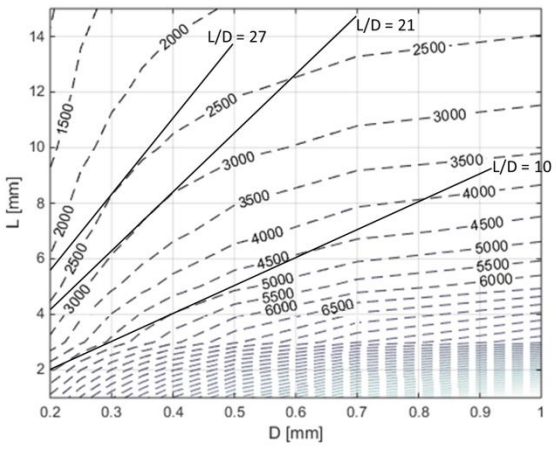

Figure 7 Cut-off frequency contour-lines on D vs L

PROBE DESIGN

Smallest possible tube diameter is selected to serve as a pitot-probe, which will stagnate the flow and deliver the total pressure up to the transducer end. Small exterior volume and hence less flow disturbance are the main concerns in the probe design. Instead of the conventional design of a pitot-probe with 90° bend, a hole is drilled on the tube in radial direction and one side is closed with a plug. That keeps the exterior geometry as a thin tube in cross flow and makes an interior geometry similar to a conventional pitot-probe. A sketch of the new pitot-tube is shown in Figure 8. Outer diameter of the tube is 0.6 mm and inner diameter is 0.35 mm. The flow volume contour is indicated with dashed lines in the figure. The pitot-tube length should be kept as short as possible. However, the final design probe is supposed to traverse in a 4 mm of gap and adding up wall thickness and assembly constraints for the probe stem, resulting tube extension from transducer tip is up to 7 mm. The cavity volume is to be kept small so that the tube interior comprises the dominating part of the total volume

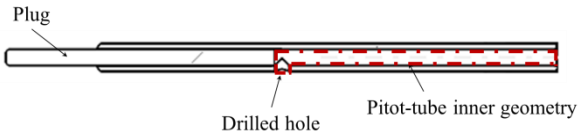

Figure 8 Pitot-tube sketch

The pitot-tube is attached to a prototype probe stem which holds a fast response miniature transducer in the vicinity of the tube end (Figure 9).

PROBE CALIBRATION

The new single-hole probe is to be used in velocity vector measurements behind an impeller. The prototype probe is initially tested for its response to direction of steady flow.

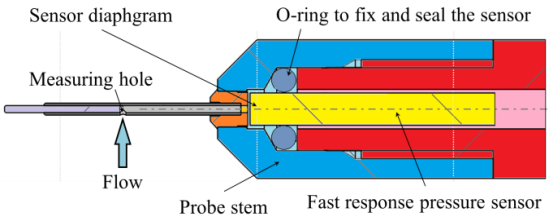

Figure 9 Pitot-tube and transducer connection

Second issue will be the distance between the measurement point and the sensor. Calibration procedure should also include a possible correction for the filtering effect of the Helmholtz resonator-like volume. However, a well-defined and fixed cavity volume is not the main concern of the initial tests.

Transducer

Kulite transducers with 1.4 mV/V/bar sensitivity are used in the probe and on the side wall of the calibration duct.

Probe response to flow direction

Calibration duct acts like a suction type wind tunnel. Air is sucked from ambient through the bell-mouth at the duct inlet. That means the total pressure of the undisturbed flow is fixed to ambient pressure. The pitot-probe is supposed to measure that pressure value when it is perfectly facing the incoming flow out of the boundary layer developing on the wall. Local static pressure is measured on a pair of wall static pressure taps aligned with the pitot-probe on both sides of the probe. The general view of the calibration duct and pressure measurement points are shown in Figure 10.

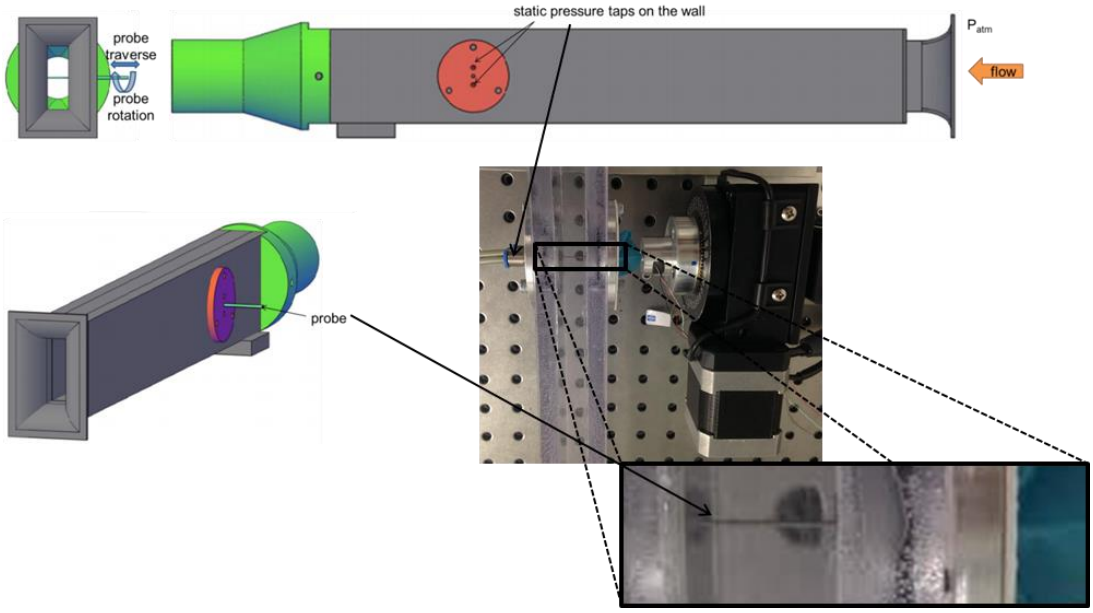

Figure 10 Pseudo-multi-hole-probe calibration duct general view

For a steady flow, probe is rotated 360° and data is acquired at every 5° of increments. Resulting pressure ratio distribution is in Figure 11. Repeatability tests are done at every 15° of increments and the error bars are on the same plot. Flow speed can be calculated for the incidence angles probe is measuring higher than the flow static pressure. When the probe measurement drops below the static pressure, it means that the sensing hole is measuring inside the flow separated from the probe body. The angle range where the probe can provide reliable flow speed data is 110° ± 3.5°.

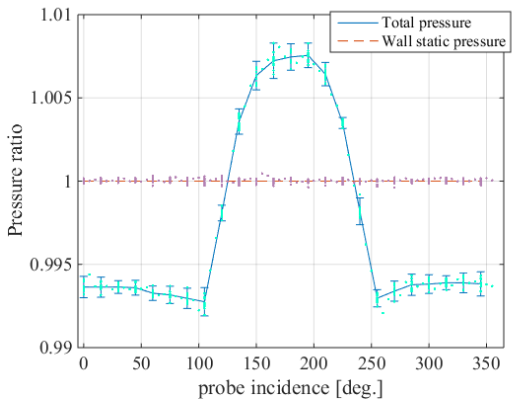

Figure 11 Probe response to flow direction

Flow speed calculated from the ratio of probe measurement to the wall static pressure is plotted in Figure 12. Negative values of speed are also represented here in order to show a complete picture from 360° scan of the probe. In three subplots, behavior of the boundary layer developing on the side walls of the duct is shown. These velocity distributions are obtained for three different incidences of the probe. For an incidence close to separation from probe body, merge of boundary layers on the side wall and the probe body show the hint of reversed flow as the $\frac{d^2u}{dy^2} \approx 0$.

Results of 360° probe scan inside the boundary layer are compared in Figure 13. Probe sensitivity to flow direction is the lowest when the measuring hole is inside the core flow. Core flow range is 30°. In order to simulate a 3-hole probe, this probe should measure from three different incidences at 35° so that the possibility of the probe to measure always out of the wake will be the highest. Because the measuring hole will not act like a Kiel probe and will measure the real total pressure only inside the core and the pressure profile will get narrower for higher flow velocities, defining a calibration map for a pseudo-3-hole probe will not be possible.

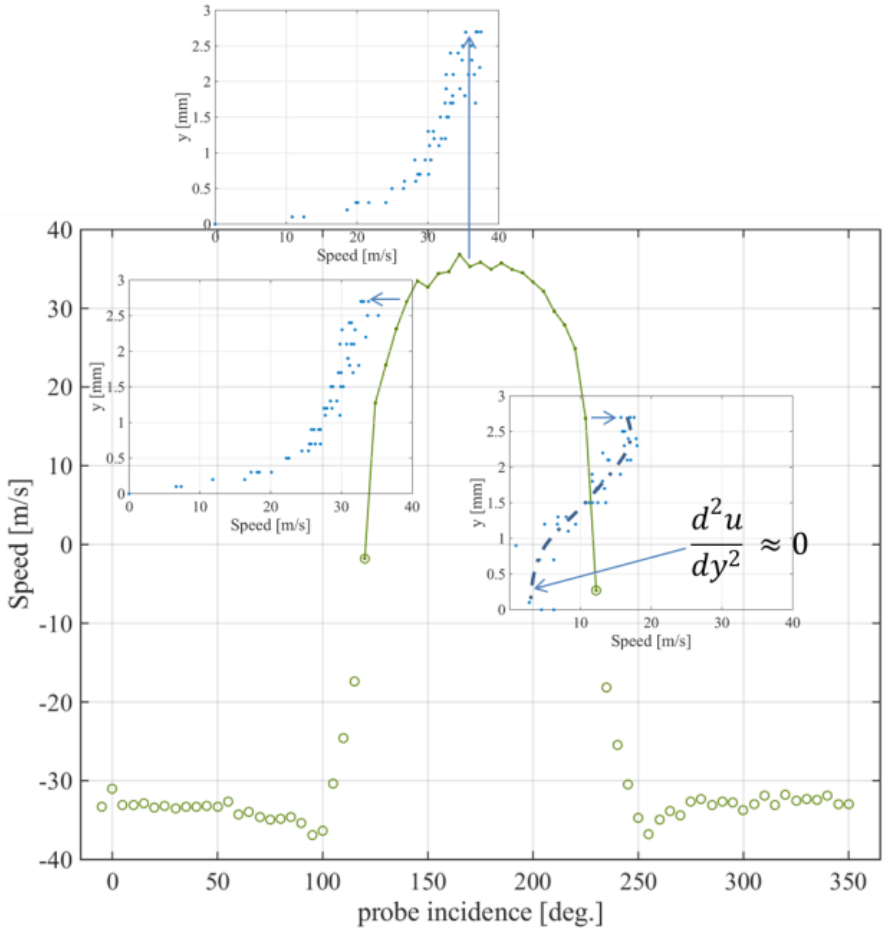

Figure 12 Flow speed calculated from probe measurements

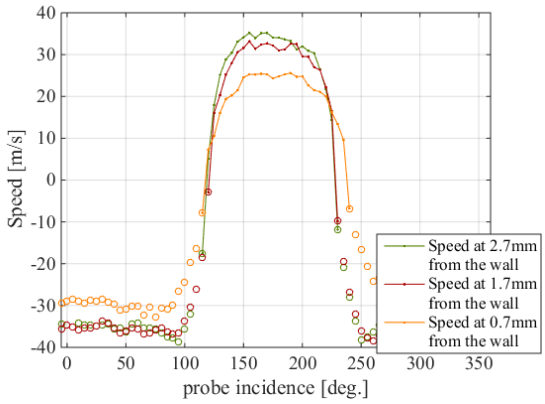

Figure 13 Flow speed inside the boundary layer

Instead, the probe will be used as in the calibration procedure and velocity vector will be determined according to a nulling method.

Probe Incidence Data Processing

Data from the 360º scanning of the probe should be processed in a way that in the absence of static pressure measurement from the wall, flow speed information is available. Flow angle will be defined as the symmetry line of the pressure distribution discarding the wake and core flows (Figure 14). Uncertainty of symmetry line is ±0.8º with 95% confidence level, according to the repeatability tests.

Flow speed can only be calculated with a correct estimation of static pressure in the lack of any wall static pressure measurement. Static pressure line passes approximately at mid-point of the core and the wake (Figure 15). Maximum deviation of core/wake mid-pressure from real static pressure is 0.1% of the real value.

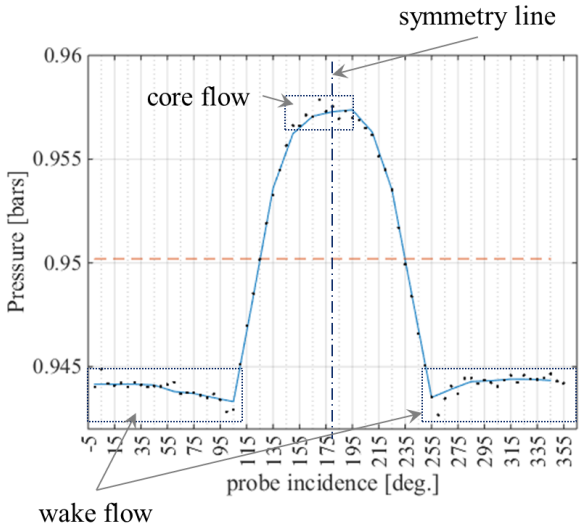

Figure 14 Flow angle as symmetry line

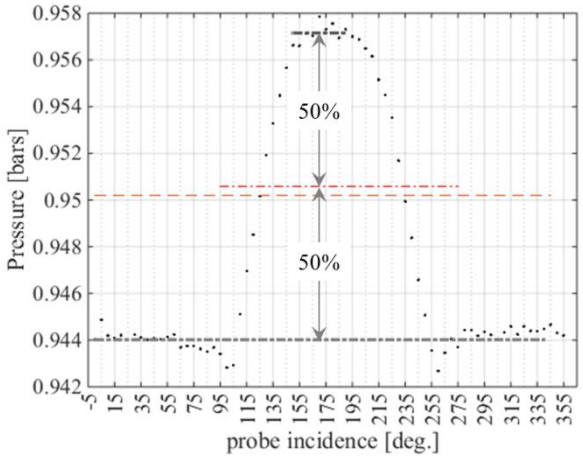

Figure 15 Static pressure as mean of core and wake pressures

Probe is tested at higher and lower flow speeds. Uncertainty in determining the speed is compared with that of the mean velocity in the duct, both for 95% confidence level, in Table 1.

Table 1 Uncertainty in flow speed

Deviation (%) in duct speed	3.2% (max.)
Error (%) in probe core speed	4% (max.)

CONCLUSION

A prototype probe is manufactured to determine flow velocity vector with minimum blockage possible. The probe comprises of a thin tube in cross flow and stem to preserve the transducer. According to a dynamic model estimating channel resonating frequencies and gains, the prototype probe will resonate around 4 kHz. Probe will require no correction or a transfer function when measuring flows fluctuating lower than 1.3 kHz.

Probe sensitivity to flow direction is proved. The probe is able to capture the pressure distribution on a cylinder in cross flow. It is also sensitive enough to capture the boundary layer behavior. It is observed that pressure data of 360º around the probe is sufficient to estimate the static pressure of the flow. Current information on the probe will be used to determine time averaged flow speed and angle at the exit of a rotating impeller. A further study is required to determine a transfer function for fluctuations at higher than the cut-off frequency of the tube.

REFERENCES

[1] J. Demierre, A. Rubino, and J. Schiffmann, “Modeling and Experimental Investigation of an Oil-Free Microcompressor-Turbine Unit for an Organic Rankine Cycle Driven Heat Pump,” *J. Eng. Gas Turbines Power ASME*, vol. 137, no. 3, 2015.

[2] A. Javed, C. Arpagaus, S. Bertsch, and J. Schiffmann, “Small-Scale Turbocompressors for Wide-Range Operation with Large Tip-Clearances for a Two-Stage Heat Pump Concept,” *Int. J. Refrig.*

[3] J. J. N. Everitt, “The role of impeller outflow conditions on the performance and stability of airfoil vaned radial diffusers,” Massachusetts Institute of Technology, 2014.

[4] M. Mansour, N. Chokani, A. I. Kalfas, and R. S. Abhari, “Time-resolved entropy measurements using a fast response entropy probe,” *Meas. Sci. Technol.*, vol. 19, no. 11, p. 115401, Nov. 2008.

[5] M. W. Schleer, *Flow structure and stability of a turbocharger centrifugal compressor*. Diss., Technische Wissenschaften, Eidgenössische Technische Hochschule ETH Zürich, Nr. 16605, 2006, 2006.

[6] Peter Kupferschmied, Pascal Köppel, Christian Roduner, and Georg Gyarmathy, “On the development and application of the fast response aerodynamic probe system in turbomachines - Part 1: The measurement system,” *J. Turbomach.*, vol. 122, pp. 505–516, Jul. 2000.

[7] M. J. Lucas, Ed., *Handbook of the acoustic characteristics of turbomachinery cavities*. New York: ASME Press, 1997.
[8] D. Allegret-Bourdon, "Experimental study of fluid-structure interactions on a generic model," 2004.
[9] H. Bergh and H. Tijdeman, "Theoretical and experimental results for the dynanmic response of pressure measuring systems," National Aero- and Astronautical Research Institute Amsterdam, NLR-TR F.238, 1965.
[10] R. Pemberton, "An overview of dynamic pressure measurement considerations." Scanivalve Corp., Mar-2010.
[11] G. Paniagua and R. Dénos, "Digital compensation of pressure sensors in the time domain," *Exp. Fluids*, vol. 32, no. 4, pp. 417–424, Apr. 2002.